



## From iron curtain to green belt: Shift from heterotrophic to autotrophic nitrogen retention in the Elbe River over 35 years of passive restoration

Alexander Wachholz<sup>1</sup>, James W Jawitz<sup>2</sup>, Dietrich Borchardt<sup>1</sup>

<sup>1</sup>Department of Aquatic Ecosystem Analysis and Management, Helmholtz-Centre for Environmental Research (UFZ), Magdeburg, Germany

5 <sup>2</sup>Soil and Water Sciences Department, University of Florida, Gainesville, FL, USA

Correspondence to: Alexander Wachholz (alexander.wachholz@uba.de)

**Abstract.** We investigate changes in in-stream nitrogen retention and metabolic processes in the River Elbe between 1978 and 2020. We analyzed multi-decadal time series data and developed a metabolic nitrogen demand model to explain trends in dissolved inorganic nitrogen (DIN) retention, gross primary production (GPP), and ecosystem respiration (ER) during a period of highly dynamic pollution pressures in the Elbe River (Central Europe). Our findings reveal a marked increase in summer DIN retention and a decrease in winter DIN retention, establishing a distinct seasonal pattern. We identified three periods in the Elbe's DIN retention dynamics: dominantly heterotrophic under high organic and inorganic pollution pressure (1980-1990), transition (1990-2003), and dominantly autotrophic with lower pollution (2003-2017). We link these changes to reduced industrial pollution, improved wastewater treatment, and a shift in the in-stream balance between heterotrophic and autotrophic processes. During the first period, high ER and heterotrophic growth efficiency contributed to elevated metabolic nitrogen demand, primarily driven by heterotrophic processes. As pollution from industrial and wastewater emissions decreased, GPP rates increased, and ER gradually declined, prompting a shift towards an autotrophic-dominated nitrogen retention regime. Our study indicates a tight coupling of nutrient reduction from external sources and dominant processes of natural attenuation in large rivers, which needs to be considered for projections of recovery trajectories toward sustainable water quality.

### 1 Introduction

Large river systems have been substantially impacted by anthropogenic pressures associated with economic development, including observed long-term trends of ecosystem degradation throughout much of the 20th century (Vörösmarty et al., 2015; Meybeck et al., 2018). However, ecosystem protection regulations promulgated in recent decades have supported the recovery of many river ecosystems (Minaudo et al., 2015; Westphal et al., 2019), including improvements in river metabolic regimes (Diamond et al., 2022a; Jarvie et al., 2022) and reduction of dissolved inorganic nitrogen loads (Wachholz et al., 2022). Much work has examined the terrestrial drivers of these multi-decadal trajectories of river ecosystems (Ehrhardt et al., 2019; Dupas et al., 2018; van Meter et al., 2017). However, little is known about the impact of those long-term changes on the in-stream processes. An important in-stream process that is susceptible to external pressures is in-stream retention of dissolved inorganic nitrogen (DIN), which plays a crucial role in watershed nitrogen (N) budgets, often retaining over 30% of the inputs (Ritz and Fischer, 2019a; Rode et al., 2016; Wang et al., 2022). This important ecosystem function also helps



protect downstream ecosystems from eutrophication (Bianchi et al., 2010) induced by highly reactive forms of nitrogen, such as nitrate and ammonium (Seitzinger et al., 2002). In-stream DIN retention is closely linked to other ecosystem functions, especially stream metabolism (Hall and Tank, 2003; Heffernan and Cohen, 2013). Long-term changes of metabolism  
35 (Arriota et al., 2019), nitrogen loading (Ballard et al., 2019), and nitrogen composition (Wachholz et al., 2022) have been observed in rivers. Here, we are interested in associated long-term patterns of in-stream DIN retention.

In-stream DIN retention is performed by algae, bacteria, and macrophytes in the water column and sediments (Deutsch et al., 2009; Middelburg and Nieuwenhuize, 2000), which either assimilate DIN into their biomass or use it for metabolic  
40 processes. The activity of these organisms is influenced by various environmental factors such as water temperature, residence time, and nutrient concentrations (Collos and Harrison, 2014a; Rasmussen et al., 2011; Snell et al., 2019). While travel time (Bertuzzo et al., 2017) and water temperature (Sherman et al., 2016) are often assumed to be the primary controls of in-stream DIN retention, the composition of DIN can also play a significant role. For instance,  $\text{NH}_4\text{-N}$  is favored over  $\text{NO}_3\text{-N}$  by many algae and bacteria (Cejudo et al., 2020). If sufficient  $\text{NH}_4\text{-N}$  is available, the DIN uptake by unicellular  
45 algae can increase by a factor of 2-16 (Collos and Harrison, 2014b). Understanding of DIN retention should also consider the relative contributions of algae, bacteria, and macrophytes, which each have preferences for different DIN species (Bergbusch et al., 2021; Collos and Harrison, 2014), incorporate N at different stoichiometric ratios into their biomass (Diamond et al., 2022; Godwin and Cotner, 2018), and have different growth efficiencies (the ratio of consumed resources that are assimilated into biomass, e.g. del Giorgio, 1997).

50 While long-term trends in the drivers and correlates with in-stream DIN retention are relatively well known (e.g. Ballard et al., 2019; Wachholz et al., 2022, Diamond et al., 2022), their consequences on in-stream DIN retention itself are understudied. This leaves considerable uncertainty in long-term watershed N budgets, which are already uncertain due to hard-to-quantify phenomena, such as time lags (Lutz et al., 2022). Therefore, we propose the following research question:  
55 How do the magnitude and dominant processes of in-stream DIN retention change in response to long-term changes in DIN composition and river trophic regime? To answer this question, we studied the Elbe River from 1978 to 2017. During this period, the Elbe river underwent a significant transition: before 1990, most of its catchment lay beyond the iron curtain and experienced significant chemical pollution, especially from heavy fertilizer use due to the agro-industrial revolution in the GDR after the 1960s (Bauerkaemper, 2004). Furthermore, large amounts of untreated wastewater from urban and industrial  
60 areas further polluted the stream (Netzband et al., 2002). However, after the GDR's collapse in 1989, industrial facilities closed, and WWTPs were rapidly constructed in the 1990s following the German reunification in 1991, resulting in decreased emissions from these sources and improved water quality in the Elbe (Adams et al., 2001). Parts of the Elbes remaining floodplain are now located within the European Green Belt with the aim to preserve its valuable functions for flood retention and biodiversity (Serra-Llobet et al., 2022).

65



Previous work suggests a shift from a heterotrophic to an autotrophic-dominated metabolic regime following the reduction of riverine biological oxygen demand in response to wastewater treatment improvements following the GDR collapse (Lehmann and Rode, 2001). However, the concomitant changes in DIN retention during this period have not been examined. Quantitative links between in-stream metabolism and nutrient retention have been described by many authors (Hall and Tank, 2003; Heffernan and Cohen, 2010; Kamjunke et al., 2021; Rode et al., 2016; Zhang et al., 2023). The N demand of GPP and ER in an ecosystem can be estimated, subject to assumptions about growth efficiencies (the share of GPP/ER that leads to biomass growth), biomass C:N ratios, and photosynthetic/respiratory quotients ( $O_2/C$  ratio during photosynthesis/respiration) (Hall and Tank, 2003a). As both auto- and heterotrophic microorganisms use DIN as their preferred N source (Rier and Stevenson, 2002) those assumptions allow us to link the DO and the DIN balance of a river segment. Other processes, however, disturb this link by influencing either DO or DIN but not both. Possible examples are other biologic processes such as nitrification (retains DO but does not affect DIN budget directly) and denitrification (removes  $NO_3-N$  but does not consume DO). However, physicochemical effects such as ad- or desorption of  $NH_4-N$  also influence the DIN budget of a river segment without affecting the DO budget (Triska et al., 1994).

We hypothesize a natural condition of strong coupling between metabolic processes and in-stream DIN retention (Heffernan and Cohen, 2013), but we expect this coupling to be weakened during phases of high pollution (such as during the late phases of the GDR before 1990), with re-emergent coupling as pollutant loads decrease (after 1990). GPP in the Elbe is mostly caused by phytoplankton (Hardenbicker et al., 2014), and its activity is closely linked to the in-stream N processes in the Elbe in recent years (Ritz and Fischer, 2019; Kamjunke et al., 2021). In-stream denitrification is assumed to be of minor importance (10%) in the Elbe, at least after the reunification (Ritz et al., 2017). The strong decrease in  $NH_4-N$  concentrations after 1990 (Adams et al., 2001a) suggests that nitrification and sorption processes play a minor role in the Elbe's DIN retention. Before 1990, in-stream oxygen concentrations were low (Lehmann and Rode, 2001), and  $NH_4-N$  concentrations were high (Adams et al., 2001b). We, therefore, expect that nitrification and denitrification occurred at relatively higher rates with weaker coupling between DIN retention and metabolic processes.

To test our hypothesis, we quantified DIN retention using a two-station mass balance approach along a 110 km, 8th-order segment of Elbe with no noteworthy tributaries. Furthermore, we quantified changes in the trophic regime in the Elbe by estimating gross primary production (GPP) and ecosystem respiration (ER) using the single-station hourly oxygen mass-balance approach (Odum, 1956). We linked in-stream DIN retention to metabolic rates using stoichiometric constraints and assessed the relative importance of autotrophic and heterotrophic processes.



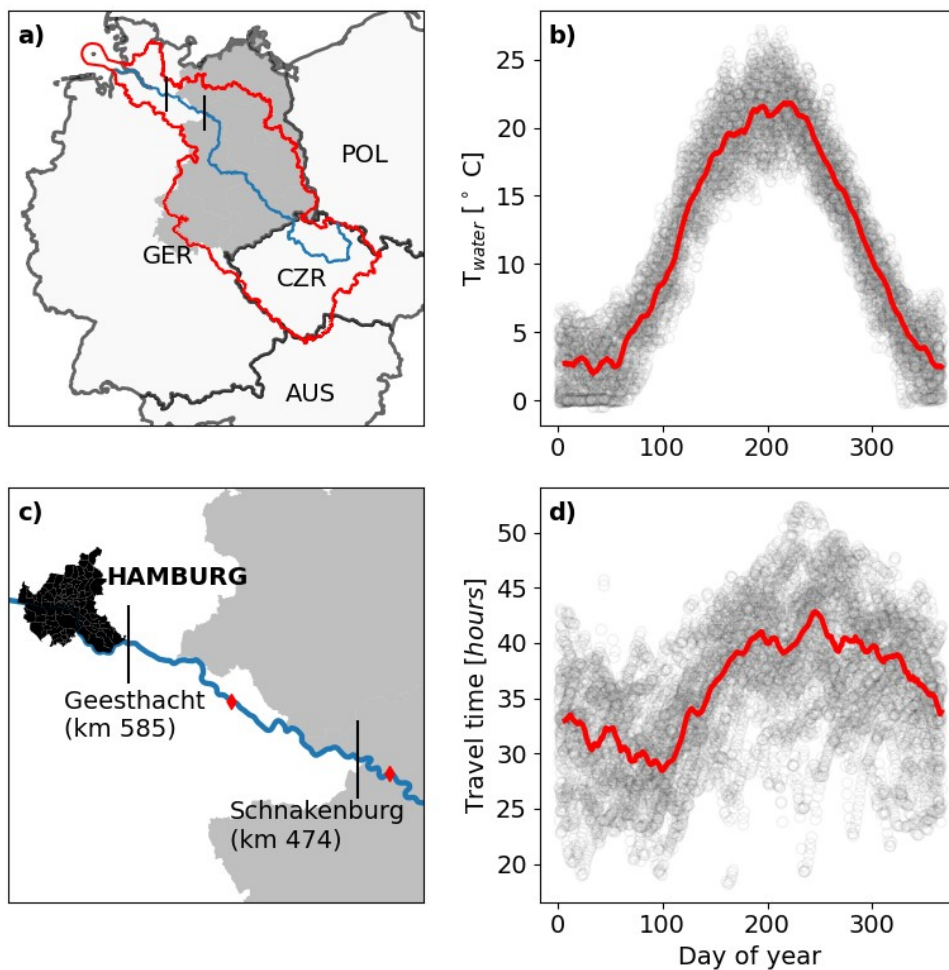
## 2 Data and methods

### 2.1 Overview

We used DIN and DO mass balances to assess the magnitude and responsible processes of in-stream DIN retention over 42 years from 1978 to 2020. We inversely modeled DO concentrations using a Bayesian method to estimate the metabolic processes over time. We linked metabolism and in-stream DIN retention using a simple model based on stoichiometric constraints and growth efficiencies.

### 2.2 Study site

We studied the last 111 km of a 1094 km long 8th-order river (Elbe, Fig.1a, b) between Schnakenburg (km 474) and Geesthacht (km 585) which was a part of the iron curtain before 1990. The studied segment has no noteworthy tributaries and is located 30 km downstream of the last larger tributary (Havel), contributing between 10 and 20% of the Elbe discharge (Fig. S1). The annual mean discharge at the downstream station Geesthacht (km 585) is 716 m<sup>3</sup>s<sup>-1</sup> (IKSE, 2005).



110 **Figure 1: Location of the investigated river segment (a, c) in Europe. The blue line marks the Elbe main stream and the red outline represents the catchment. Black vertical lines mark the beginning and the end of the segment (sampling locations). Red diamonds in panel c indicate discharge gages. The former area of the German Democratic Republic (GDR) is represented by the grey shade. Intra-annual patterns of water temperature (b) and travel time (d). Circles show raw data, and red lines multi-year 7 day running means for each day of the year.**

### 115 2.3 Two-station mass-balance

For the quantification of in-stream DIN retention, we use a two-station mass balance approach (e.g., Ritz and Fischer, 2019a). The upstream site (Schnackenburg) is located at stream kilometer 774 and has weekly (1978-1991) and bi-weekly (1991-2021) water quality ( $\text{NO}_3\text{-N}$  and  $\text{NH}_4\text{-N}$ ) time series available. Nitrite ( $\text{NO}_2\text{-N}$ ) was not considered as, even in high nitrogen pollution periods, it made up between 1 and 3% of the DIN for both input and output (Fig. S2). The downstream



120 site (Geesthacht) at stream km 885 has weekly  $\text{NO}_3\text{-N}$  and  $\text{NH}_4\text{-N}$  from 1980-1988, bi-weekly until 2006, and monthly  
afterward. A data gap from 1988-1993 was filled with data from another sampling site located at stream km 598  
(Zollenspieker), as described in Wachholz et al. (2022). The discharge gage (Neu Darchau) is located 50 km downstream of  
the sampling site used to estimate DIN load (station Geesthacht). However, the difference in catchment area between the  
125 sampling site and the gage is less than 3% (Wachholz et al., 2022). We consider this by assuming a 10 % error in discharge  
measurements in our uncertainty propagation, while a previous mass balance study (Ritz and Fischer, 2019) assumed the  
errors to be  $\leq 5\%$  in the Elbe.

### 2.3.1 WRTDS model

To reconcile differences in sampling dates between the upstream and downstream stations, daily loads of  $\text{NO}_3\text{-N}$  and  $\text{NH}_4\text{-N}$   
were estimated using the weighted regression on time, discharge, and season (WRTDS) function of the R package EGRET  
130 (Hirsch et al., 2010). The WRTDS function uses a weighted regression approach to estimate daily loads and concentrations,  
accounting for non-linearity and non-stationarity in the relationships between the time, discharge, season, and concentrations  
over time. Measured and simulated daily concentrations showed very good agreement ( $R^2 > 0.7$  and percent bias  $< 3$ , see Fig.  
S3).

### 135 2.3.2 Retention metrics

Using the daily loads provided by the WRTDS function, we calculated in-stream DIN retention  $R_{\text{obs}}$  as

$$R_{\text{obs}} = L_{\text{in}} - L_{\text{out}} \quad (\text{I})$$

where  $L$  is the DIN load [ $\text{kg day}^{-1}$ ]. Uncertainty in  $R_{\text{obs}}$ , was computed based on Gaussian error propagation (Section S2). We  
140 then calculate the relative retention  $RR$

$$RR_{\text{obs}} = \frac{R_{\text{obs}}}{L_{\text{in}}} \quad (\text{II})$$

and the area weighted retention  $U$  [ $\text{kg d}^{-1}\text{m}^{-2}$ ]

$$U_{\text{obs}} = \frac{R_{\text{obs}}}{A} \quad (\text{III})$$

where  $A$  [ $\text{m}^2$ ] is the bottom area of the river segment (Stream Solute Workshop, 1990). We calculate  $R_{\text{obs}}$ ,  $RR_{\text{obs}}$ , and  $U_{\text{obs}}$   
145 for both DIN and  $\text{NH}_4\text{-N}$ . We corrected the  $L_{\text{out}}$  time series for travel time to align the inflow and outflow time series. The  
estimated travel times for the segment ranged from 19 and 52 hours (Fig. 1d), but since loads were only available as daily  
means, we evaluated corrections in increments of days (Table SI-1), and we found that shifting  $L_{\text{out}}$  one day ahead of the  $L_{\text{in}}$   
series yielded the best results when a discharge mass balance was considered.



## 150 2.4 Metabolism estimations

The single station method for metabolism estimation in rivers with Bayesian inference involves using dissolved oxygen (DO) data from a single monitoring station to estimate the rates of gross primary production (GPP) and ecosystem respiration (ER) in the river (e.g., Hall et al., 2016).

$$DO_{t+\Delta t} = DO_t + \frac{gpp}{par} PPF D - er \Delta t + \frac{k 600 \left( \frac{Sc}{600} \right)^{\left( -\frac{1}{2} \right)} (DO_{max} - DO_t)}{z} \Delta t \quad (IV)$$

155

where  $gpp$  and  $er$  are the daily rates [ $\text{mmol m}^{-3} \text{d}^{-1}$ ] of the respective parameters,  $PPFD$  is the photosynthetic photon flux density [ $\mu\text{mol m}^{-3} \text{d}^{-1}$ ],  $k600$  is the gas exchange coefficient [ $\text{m d}^{-1}$ ],  $Sc$  is the dimensionless Schmidt number (Wanninkhof, 1992) which is calculated based on water temperature,  $DO_t$  and  $DO_{max}$  are the actual and maximum (at 100% saturation) DO concentrations [ $\mu\text{mol l}^{-1}$ ], and  $z$  is the channel depth [m]. The implementation of the Bayesian inference model to solve Eq.

160 IV can be found in Section S4.

## 2.5 Channel geometry estimations

Calculating area-weighted retention rates and inverse modeling of in-stream metabolism for a river segment requires knowledge of the surface area, water residence times, and channel depth. The methods to obtain these estimates are summarized below but are described in detail and validated in Section S1 and Fig. S4. We used discharge-based transfer  
165 functions to estimate the geometrical parameters at different water levels (e.g., Booker and Dunbar, 2008). We estimated travel time  $\tau$  using a transfer function proposed by (Scharfe et al., 2009) for the German Elbe. For the channel area of the investigated segment, we established a transfer function based on discharge, which we parametrized with channel areas derived at different discharge conditions from Sentinel 2 images with a surface water detection algorithm (Normalized Difference water index). We employed a power law model for the channel depth based on data from Aberle et al. (2010).

## 170 2.6 Data Preparation

Implementation of Eq. IV requires hourly estimates of  $PPFD$ ,  $DO$ ,  $DO_{max}$ ,  $z$ , and  $Sc$ . We interpolated diurnal DO concentrations by fitting sine functions to a time series of daily mean, minimum, and maximum values from 1978 to 2017, as described in Section S3. Simulated DO concentrations were validated with two years of hourly measured values showing characteristics of a good fit ( $R^2=0.96$ ,  $RMSE=0.42 \text{ mg l}^{-1}$ ). We estimate hourly solar radiation (as  $PPFD$ ) based on the  
175 method proposed by Duffie and Beckman (2013), which is implemented in the Python package *solarPy*. We calculate DO saturation based on the method of Weiss (1970) using hourly air pressure data from the German weather service (DWD)



station Seehausen (ID 4642) and daily mean water temperature measured together with the *DO* data. To estimate the effects of using daily instead of hourly water temperature measurements, we calculated the mean diurnal temperature variability from 24 years of hourly water temperature in the Elbe, which is 1.1 deg C (+- 0.7). For typical *DO*, *T*, and *p* conditions at the Elbe, this can lead to a deviation in  $DO_{sat}$  of a maximum of 5.4 % (see Fig. S5), which we neglect in the following analysis.

## 2.7 Estimating the N demand of metabolic processes

The demand of N caused by GPP and ER can be estimated based on the respective organisms' growth efficiency (*GE*), the photosynthetic- and respiratory quotient (*PQ*, *RQ*), and the C:N ratio of their biomass (e.g., (Hall and Tank, 2003a). *GE* [-] describes the proportion of resources and energy that is captured by photosynthesis ( $GE_{AUTO}$ ) or respiration ( $GE_{HET}$ ) that is incorporated into new biomass (del Giorgio et al., 1997; Hall and Tank, 2003b). *PQ* and *RQ* describe the ratio of  $O_2$  produced/ consumed per  $CO_2$  consumed/ produced (Berggren et al., 2012; Hall and Tank, 2003a). Those two concepts can be used to assess how much C is incorporated into biomass for any given GPP and ER rate. Via the C:N ratio of the biomass, the N demand can then be estimated. Since autotrophic and heterotrophic microbes prefer DIN to other forms of nitrogen (Reer and Stevenson, 2002) and DIN is always available at concentrations  $> 1 \text{ mg l}^{-1}$ , we interpret the N demand as DIN demand.

For autotrophic processes, we can formulate the following

$$U_{AUT}(t) = GPP(t) PQ \frac{GE_{AUT}}{CN_{AUT}} \quad (V)$$

where  $U_{AUT}$  [ $\text{mol m}^{-2} \text{ day}^{-1}$ ] is the DIN demand of the GPP rate [ $\text{mol m}^{-3} \text{ day}^{-1}$ ], and *PQ* [ $\text{mol C mol}^{-1} O_2$ ],  $GE_{AUT}$  is the autotrophic growth efficiency [-],  $C:N_{AUTO}$  is the carbon to nitrogen ratio in the autotrophic biomass and *z* is the channel depth [m] used to convert volumetric GPP to areal retention rates. Similarly, we can formulate for heterotrophic processes

$$U_{HET}(t) = R_{het}(t) RQ \frac{GE_{HET}}{CN_{HET}} \quad (VI)$$

however, it is well known that the measured ER not only caused by heterotrophic bacteria (e.g. Hall and Tank, 2003). A way to correct autotrophic respiration is to subtract the non-biomass-producing fraction of GPP from ER (Hall and Tank, 2003b).

$$R_{het}(t) = ER(t) - GE_{AUT} GPP(t) \quad (VII)$$

combining Eq. V, VI, and VII allows us to estimate the complete metabolic N demand  $U_{met}$  as follows

$$(VIII) U_{met}(t) = \left( GPP(t) PQ \frac{GE_{AUTO}}{CN_{AUTO}} + (ER(t) - GE_{AUTO} GPP(t)) RQ \frac{GE_{HET}}{CN_{HET}} \right) z(t) \quad (VIII)$$

A recent study found that the C:N of phytoplankton biomass in the Elbe is around 7.3 (Kamjunke et al., 2021) and we applied the often used  $PQ = 1$  and  $GE_{AUTO} = 0.5$  (Hall and Tank, 2003b; Heffernan and Cohen, 2010; Rode et al., 2016). We





used  $C:N_{HET} = 4.8$ , the median ratio for aquatic bacteria presented by (Godwin and Cotner, 2018), and  $RQ = 1.2$  (Berggren et al., 2012).  $GE_{HET}$ , on the other hand, is known to vary between 0.05 and 0.4 in freshwater ecosystems, with higher values under higher levels of organic pollution (del Giorgio et al., 1997). We fit Eq. VIII to  $U_{obs}$  data and only allow  $GE_{HET}$  to be variable. Although variability in  $C:N_{HET}$  and  $RQ$  can be expected, we argue that the pollution gradient in  $GE_{HET}$  gives a strong  
210 indication for being variable over the time series. Furthermore, variability in  $C:N_{HET}$  and  $RQ$  could be covered by variability in  $GE_{HET}$ , which we considered when interpreting the  $GE_{HET}$  parameter.

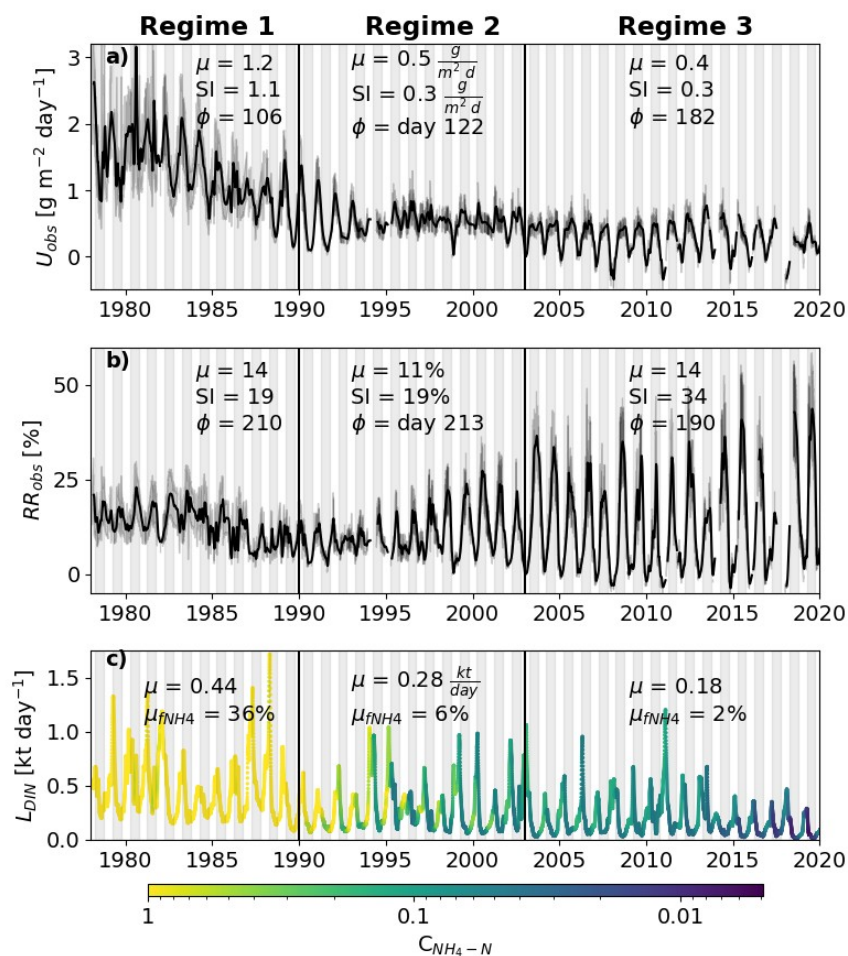
We fit Eq. VIII to the time series data for three periods, which corresponds to changes in the seasonality and magnitude of  $U_{obs}$ : 1980-1990, 1991-2002, 2003-2016 using the *curve\_fit* method implemented in the python package SciPy (Virtanen et al., 2020) and constrain  $GE_{HET}$  between 0.05 and 1. To assess the variability of  $GE_{HET}$  towards highly influential data points,  
215 we perform the fitting for 100 randomly selected subsamples with 25 % of the original data. As the  $GE_{HET}$  values generated by this approach follow a normal distribution, we use their mean and standard deviation to describe their variability for uncertainty quantification.

As  $U_{obs}$  and  $U_{met}$  values have relatively high uncertainties during Regime 1 (Fig. 2; Fig. S9b), we chose a seasonality-based validation approach for the metabolic N demand model. For the  $U_{obs}$  and  $U_{met}$  time series, we compared the annual mean ( $\mu$ ),  
220 the day of the peak ( $\phi$ ), and the seasonality index ( $SI$ ). We used a Monte Carlo approach to propagate the uncertainties of the fitted parameters GPP, ER, and  $GE_{HET}$  into the seasonality metrics. For each day where GPP, ER, and  $GE_{HET}$  estimates are available, we calculated daily minimum and maximum  $U_{met}$  values using the 90% confidence intervals determined from 100 random errors from the normal distributions defined by the daily mean and standard deviation of the respective parameter. We define minimum and maximum  $\mu$  and  $SI$  values for each year based on these confidence intervals. For the day of the  
225 peak ( $\phi$ ), we analyze the time series of the 5th, 50th, and 95th percentile of  $U_{met}$  values for each year and report the earliest (lowest), mean, and latest (largest)  $\phi$ . For  $U_{obs}$ , we repeat the same procedure, only that the basis for the error distribution is the Gaussian mass balance error propagation described in Section 3.3.2.



### 3. Results and Discussion

230



235

240

**Figure 2:** Area-weighted ( $U_{obs}$ , panel a) and relative dissolved inorganic nitrogen (DIN) retention rates ( $RR_{obs}$ , panel b) estimated using a two-station mass balance approach. The three black vertical lines correspond to the major changes in  $U$ : Regime 1 shows high mean ( $\mu$ ), strong seasonal amplitude (SI) and peaks during spring ( $\Phi = \text{day } 106$ ). Regime 3 has a much lower  $\mu$  and SI, while the day of the peak occurs during summer ( $\Phi = 182$ ). Regime 2 represents the transition between both. The black lines represent a 30 day moving average value, the shaded area around the black line shows raw values with a 90 % confidence interval. Panel c) shows the DIN load ( $L$ ) received by the investigated segment of the Elbe. The color represents the corresponding ammonium concentration.  $\mu_{fNH_4}$  is the mean fraction of DIN that consists of ammonium. The white background represent the colder six month of the year (October-April) and dark background the warmer six.



### 3.1 DIN retention

The highest  $U_{obs}$  values during the entire time series were observed during regime 1 (1978-1990), oscillating between 1 and 2  $\text{g m}^{-2} \text{d}^{-1}$  (Fig. 2a). Starting in mid of regime 1,  $U_{obs}$  decreased and oscillated mostly between 0 and 1 for the rest of the time series, with some negative values occurring during the winter in three years (2008, 2011, and 2018). During regime 1,  $U_{obs}$  peaked shortly before the vegetation period (days 106-122) and showed clear summer peaks (day 182) afterward. Peaks outside the warmer half of the year were not expected as water temperatures (Sherman et al., 2016) and residence times (Bertuzzo et al., 2017), considered the main drivers of in-stream DIN retention, are lower during this period. Furthermore, the amplitude of the oscillation ( $SI$ ) decreased after 1990 and remains constant for the rest of the time series.

The relative retention, however, showed a consistent summer peak during the entire time series (days 190-220) while the amplitude increased in regimes 2 and 3 (19 to 34) (Figure 2b).

Annual mean loads decreased throughout all three regimes from 0.44 to 0.18  $\text{kt day}^{-1}$  with a substantial decrease in annual minima around 1989 (Figure 2c). This coincided with the collapse of the GDR economy, which led to an immediate decrease in the inorganic and organic pollution of the River Elbe (Adams et al., 2001b). Likewise, the share of  $\text{NH}_4\text{-N}$  from the DIN load declined from 36 to 6%. Concentrations of  $\text{NH}_4\text{-N}$  did not reach values  $> 1 \text{ mg l}^{-1}$  later in regime 2. This slower response could reflect the long-term improvements in wastewater treatment that followed the German reunification in 1990 (IKSE, 2010). This is further supported by the fact that  $\text{NH}_4\text{-N}$  concentrations first decreased during the summer months, where dilution capabilities are lower, and the inputs from point sources play larger roles for the Elbes N regime (Wachholz et al., 2022).

Increases in area-weighted DIN retention of large rivers due to higher DIN pollution have already been reported by Kelly et al. (2021). They also remarked on changes in the drivers of  $U_{obs}$ , which reached high values even during the cold season during phases of high pollution, which agrees with our observations.

During regime 3,  $U_{obs}$  shows a stable pattern with peaks coinciding with high water temperatures and residence times (Fig. 1b, c). As neither temperature nor discharge exhibited noteworthy trends in seasonality in the Elbe during this period (Markovic et al., 2013; Mudersbach et al., 2016), we interpret this seasonality change as an indicator of a change in other driving processes, possibly in the responsible organisms. While the DIN input has a constant seasonal pattern, its magnitude and composition (share of  $\text{NH}_4\text{-N}$ ) changed remarkably throughout the time series (Figure 2c). As biota, such as algae, are known to form their assemblages according to environmental factors such as light, temperature, and nutrient availability (Snell et al., 2019), a biotic regime shift could have contributed to the  $U_{obs}$  changes.



## 270 3.2 Metabolism

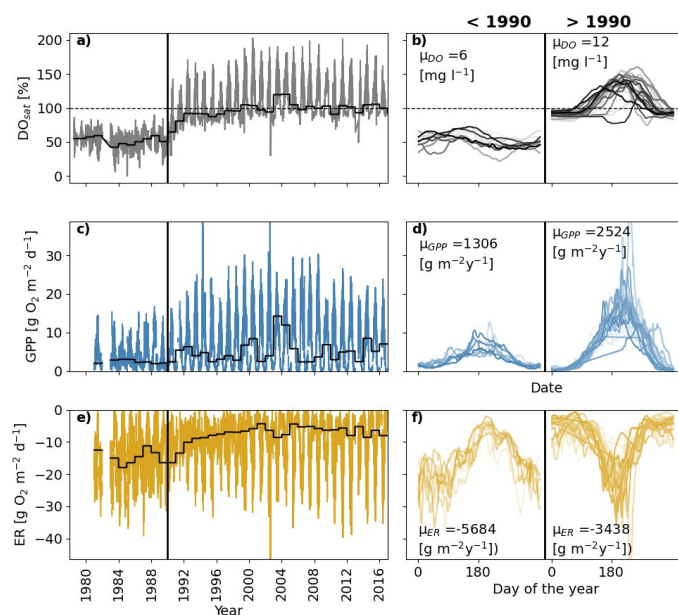


**Figure 3.** Time series of daily dissolved oxygen saturation ( $DO_{sat}$  a), daily gross primary production estimates (GPP, c), and ecosystem respiration estimates (ER, e). The black lines show the annual median  $DO_{sat}$ , GPP and ER values. Panels b, d, and f show the intra-annual patterns (30-day moving means) for  $DO_{sat}$ , GPP, and ER, each before and after 1990.  $\mu$  represents the annual mean values.

### 275 3.2.1 $DO_{sat}$

The multi-decadal pattern of DO in the Elbe showed distinct behavior before and after 1990, coinciding with the German reunification (Figure 3a). Oxygen saturation before 1990 oscillated between 20 and 70%, but increased rapidly after 1990, reaching super-saturation for the first time in 1991. Before 1990 there was no clear intra-annual pattern (Figure 2b), but for the rest of the time series,  $DO_{sat}$  oscillated seasonally between ~80 and ~180%, peaking around day 180, coinciding with the annual peaks of residence time, water temperature, and area-weighted DIN retention (Fig. 1b, c; Fig. 2a). It is well understood that the oxygen budget of the Elbe after 1990 is controlled by primary production, which rapidly increased after 1990 (Lehmann and Rode, 2001; Petersen and Callies, 2002). The absence of super-saturation before 1990 could be related to high concentrations of suspended sediments, which are known to limit GPP in rivers (Trentman et al., 2022), and which were observed to decrease in the Elbe following the improvements in wastewater treatment after 1990 (Hillebrand et al., 2018). But toxic effects from industrial waste also seem plausible, as concentrations for many organic and inorganic pollutants rapidly decreased around 1990 (Adams et al., 2001a). However, a lack of primary production would not explain the significant saturation deficit of DO before 1990. From a mass balance perspective, high rates of ER could have caused that phenomenon. Higher ER rates could have been supported by high loads of organic pollutants (Adams et al., 1996).



Further assessment of this requires the estimation of Elbe's metabolic processes which we carried out with a Bayesian model.  
290 Overall, the simulation of the DO time series with the Bayesian model showed a high agreement with observed data and high internal consistency. A detailed description of the validation can be found in the Section S4.

### 3.2.2 Gross primary production

Similar to  $DO_{sat}$ , GPP showed a clear change around 1990 with low annual peaks ( $\sim 12 \text{ g O}_2 \text{ m}^{-2} \text{ day}^{-1}$ ) before and higher ( $\sim 25 \text{ g O}_2 \text{ m}^{-2} \text{ day}^{-1}$ ) in the following years (Fig 3c). Compared to  $DO_{sat}$ , the timing of the GPP peak stayed similar throughout the  
295 time series ( $\sim$  day 190, Fig 3d), which suggests constant drivers but some sort of limitation before 1990. It is well known that light and flow regimes control the metabolism of rivers (Bernhardt et al., 2022), so the peak during high temperature and residence times is to be expected and suggests another limiting factor before 1990 (e.g., high light attenuation from suspended sediments delivered by WWTP effluents). In terms of the overall productivity of the Elbe, GPP peaks are similar to those reported in other large rivers, such as the Seine and Thames (Escoffier et al., 2018; Pathak et al., 2022).

### 300 3.2.3 Ecosystem Respiration

In contrast to GPP, ER showed peaks of similar height throughout the time series while the seasonal pattern was changed entirely (Fig 3e, f). Before 1990, ER showed high values during winter, spring, and fall, while summer values were relatively low (roughly similar to GPP values during summer, Fig. 3 e, d). After 1990, the seasonal pattern changed and gradually became more similar to GPP. Furthermore, annual mean ER rates decreased by 40 % after 1990. Before  $\sim 2000$ , the ER time  
305 series also seems more to be stochastic, but with a clear seasonal pattern emerging later on (Fig. 3e). Passive restoration of impaired rivers has been observed to contribute to the re-alignment of GPP and ER (Jarvie et al., 2022), as well as the reduction of ER rates (Arroita et al., 2019). While recent annual mean ER rates in the Elbe are similar to those of other European rivers (e.g., Loire:  $3000 \text{ g O}_2 \text{ m}^{-2} \text{ year}^{-1}$ , Diamond et al., (2022b); ) and peak ER values before 1990 are well in range of other observations (e.g., Tromboni et al., 2022), such drastic changes of ER seasonality have not yet been reported  
310 to our knowledge. However, one must consider the term 'er' from Eq. IV contains all processes that negatively impact the DO balance, including nitrification.  $\text{NH}_4\text{-N}$  was present in high concentrations in the River Elbe before 1990 (Figure 2c). At least from lakes, it is well known that nitrification can significantly contribute to oxygen depletion (Powers et al., 2017) and that nitrification rates increase with  $\text{NH}_4\text{-N}$  concentrations during cold periods (Cavaliere and Baulch, 2019) but it is unclear how that translates to rivers.

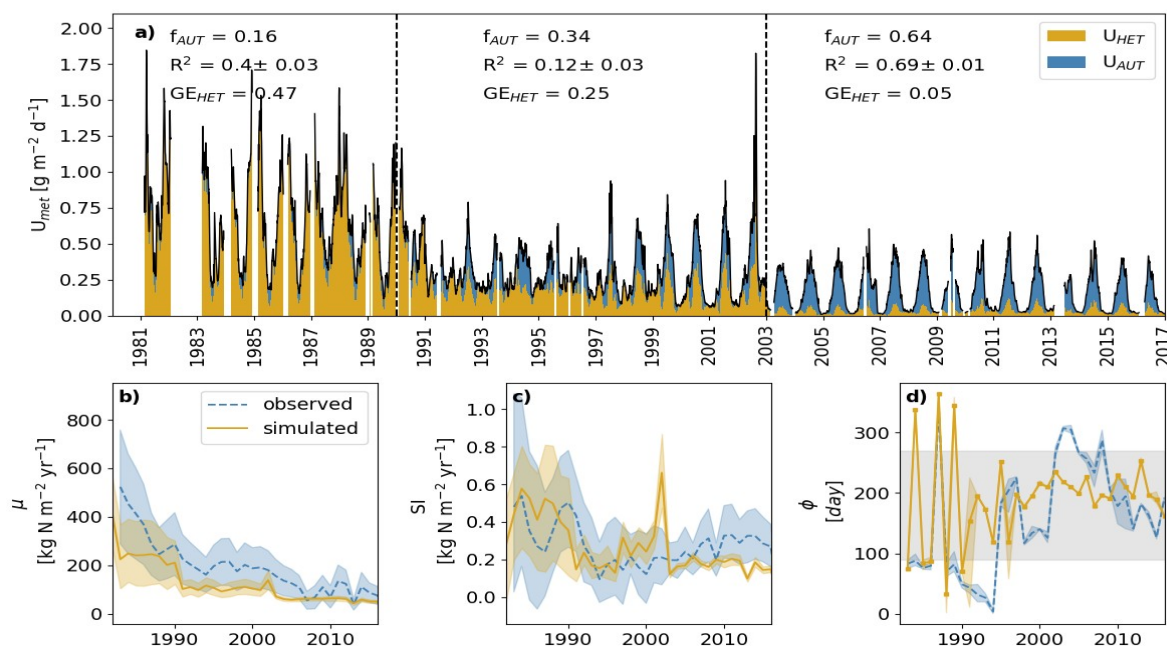
315 Note that while GPP showed a change-point-like behavior around 1990, changes in ER were more gradual (Fig. 3f). This could reflect the gradual improvements in wastewater treatment that occurred throughout the 1990s until the early 2000s (Adams et al., 2001a; Wachholz et al., 2022). This leads us to speculate that the limitation of GPP before 1990 was more closely linked to the industrial wastewater discharges, which rapidly ceased around 1990 (Adams et al., 1996), while the high ER rates were supported by domestic wastewater.

320



Considering annual mean net ecosystem productivity ( $NEP = GPP - ER$ ), the Elbe is a net-heterotrophic system throughout the time series, which means more  $O_2$  is consumed than produced. This is predicted by the river continuum concept for large rivers (Strahler order  $> 6$ , Vannote et al., 1980). Before 1990, however, high ER and low GPP rates led to an annual  $DO$  deficit of  $\sim 4400 \text{ g } O_2 \text{ m}^{-2} \text{ year}^{-1}$ . After 1990, this was reduced to  $\sim 900 \text{ g } O_2 \text{ m}^{-2} \text{ year}^{-1}$ .

### 325 3.3 Linking Metabolism and DIN retention



330 **Figure 4. (a) Time series of area-weighted DIN retention as predicted by the metabolic N demand model (dark line). Colors represent the fraction caused by the N demand of GPP ( $U_{HET}$ ) and ER ( $U_{AUT}$ ).  $f_{AUT}$  is the mean  $U_{AUT}/U_{met}$  for the three periods separated by dashed lines.  $GE_{HET}$  is the fitted heterotrophic growth efficiency and  $R^2$  coefficient of determination of the model fits. Gaps in the time series result from dates where no reasonable metabolism rates could be established. (b, c, d) Seasonality-based validation of the metabolic N demand model. The three seasonality metrics (annual mean  $\mu$  (a), seasonality index SI (b), and day of the peak  $\phi$  (c)) are shown for both observed and simulated area-weighted DIN retention. The shaded areas mark the 90% confidence interval resulting from a Monte Carlo-based error propagation. The dark shaded area in c) represents the warmer half of the year, corresponding to Fig.2. Panel d) shows the distributions of the and the coefficient of determination  $R^2$  for the three periods that were used for fitting the model.**

340 Despite its conceptual nature, the metabolic N demand model showed promising results (Figure 4a-d). The confidence intervals of most seasonality metrics overlap between simulated and observed for almost the entire time series. The model consistently underestimated the observed annual mean ( $\mu$ ), but the overall tendency of decreasing values is well captured. The observed amplitude metric SI is well predicted by the model during regimes 1 and 2, but is underpredicted during regime 3. This could be caused by the negative  $U_{obs}$  values, which cannot be captured by the model as all terms in Eq. VIII are positive. For the day of the peak ( $\phi$ ), the confidence intervals did not always overlap, but again, the general tendency of  $\phi$



occurring during the cold season before 1990 and  $\phi$  during the warm season (shaded area) after 1990 is well represented by the model (Fig 4d). The  $GE_{HET}$  parameter decreases between all three regimes with minimal variability inside the regimes (Fig 4a). In the first period (1980-1990),  $GE_{HET}$  was higher than previously reported values ( $\leq 0.4$  from del Giorgio et al., 1997). It has to be acknowledged that variability of the terms  $C:N_{HET}$  and  $RQ$  of Eq. VIII could also contribute to the fits. After 2003,  $GE_{HET}$  was reduced to the minimum allowed value of 0.05. This reduction fits overall well with the ammonium concentrations in the Elbe (Fig 2c), which were still relatively high (mean of  $0.4 \text{ mg l}^{-1}$  between 1990 and 2002) before they reached present low levels (mean of  $< 0.06 \text{ mg l}^{-1}$ ). The  $R^2$  comparing  $U_{obs}$  and  $U_{met}$  values is generally low during Regimes 1 and 2, reaching  $\sim 0.7$  in 2003-2017.

Fitting the metabolic N demand model allowed us to differentiate which share of in-stream DIN retention is caused by auto- ( $U_{AUT}$ ) and heterotrophs ( $U_{HET}$ ).  $U_{AUT}$  and  $U_{HET}$  show a clear trend over the investigated time period (Fig 5). During the 1980s, almost all metabolic N demand came from  $U_{HET}$  (84%), and only during summer/ fall did significant shares of  $U_{AUT}$  become visible. This relates well to observations of the low GPP rates before 1990 (Fig 3c, d), which should have translated into little  $U_{AUT}$  because little N is needed to support the low GPP rates. Before 1990, ER and  $GE_{HET}$  were very high, leading to an overall high metabolic N demand consistent with high  $U_{obs}$  values (e.g., Fig 4b). From 1990 until 2003,  $U_{HET}$  was still dominant for most of the year (66% of  $U_{met}$ ), with summer peaks in  $U_{AUT}$ . After 1997, the seasonality of  $U_{HET}$  and  $U_{AUT}$  aligned. After 2003,  $U_{AUT}$  comprised most of  $U_{met}$  (64%). The river segment, however, remained net-heterotrophic (annual mean  $ER > GPP$ , Fig 3 d, f), but according to our results, little of that heterotrophic activity results in the assimilation of DIN into biomass ( $GE_{HET} = 0.05$ , Fig 3d). However, the low  $GE_{HET}$  value cannot be exclusively interpreted as a sign of low heterotrophic growth efficiency, as an increase in the heterotrophic C:N ratio (biomass with less N per C) could have the same effect on Eq. VIII. To facilitate the observed decrease in  $U$ , the C:N ratio of the heterotrophic biomass must have reached 50, while usually values in the range of 1 to 20 are being discussed (Godwin and Cotner, 2018). However, a combined increase in biomass C:N ratio and decreased growth efficiency seems plausible. This would not affect our interpretation as both the increased C:N ratio and decreased growth efficiencies represent a limited N demand of in-stream heterotrophic activity.

The model validation based on seasonality metrics suggested good model performance. Robust  $R^2$  values were found only for the last period (2003-2017). While the seasonality-based validation considers the uncertainty in  $U_{met}$  and  $U_{obs}$  and compares the seasonal patterns, the  $R^2$  compares actual  $U$  values. Considering our hypothesis, we interpret this as follows: While the seasonal patterns were consistently well represented by the  $U_{met}$  model, the  $R^2$  reflects the strength of the coupling between the metabolic processes and the in-stream DIN retention. This only happened after ER developed a pattern following GPP (Fig. 3e). As the seasonal patterns of ER and GPP are well aligned during the period of high  $R^2$  (Fig. 3d, f), we conclude they are now controlled by the same processes, (residence time and temperature/ light). ER is often higher during phases of higher organic pollution loads (Arroita et al., 2019; Jarvie et al., 2022) as it is supported by organic substances from sewage. We speculate that the ER during regime 3 depended more on autochthonous organic matter production from phytoplankton.



In summary, we explain the trends in  $U$  as follows: During regime 1 (1978-1990), the Elbe received high loads of particulate, organic, and inorganic pollution, which resulted in high ER and low GPP values. High ER and  $GE_{HET}$  values led to high metabolic N demand with a stochastic seasonal pattern driven by the ER mostly. High nitrification and possibly denitrification rates led to a weaker coupling of metabolic processes and  $U$ , which was still evident when seasonal patterns were used for validation. After the rapid decrease in industrial pollution around 1990, GPP rates increased swiftly while ER decreased gradually in response to improvements in wastewater treatment. This led to a transition from a heterotrophic to an autotrophic-dominated DIN retention regime. Summer  $U$  increases fast while winter  $U$  decreases slowly, which leads to a reduced seasonal amplitude of  $U$ . Further improvements in wastewater treatment gradually remove the support for high ER rates, which become more dependent on the autochthonous organic material, leading to coinciding peaks of ER and GPP we see during regime 3. These coinciding peaks propagate into high  $U$  values during summer and low during winter, which we observe for the rest of the time series. A strong coupling emerges as the processes that decouple metabolism and DIN retention lose importance (nitrification, denitrification).

### 3.4 Ecological implications

Long-term changes in GPP and ER can have a multitude of ecological implications for the river segment itself or downstream ecosystems. For example, high ER and low GPP, as we observed in the Elbe before 1990, can lead to increased riverine  $CO_2$  emissions (Attemeyer et al., 2021). Higher primary production in the Elbe after 1990 caused greater export of organic matter to the estuary during summer, which supports higher rates of estuarine ecosystem respiration, which in turn decreases DO concentrations (Amann et al., 2012), which can reduce available habitats for fish species (Mann, 1996).

The changed seasonality of DIN retention also likely had an impact on downstream ecosystems. Even though absolute retention rates before 1990 were higher (Fig. 2a), only 20-25 % of DIN was retained during summer (Fig. 2b), when algal blooms are most likely to occur. After the German reunification, the decreased DIN load (Fig. 2c) and increased in-stream retention led to less DIN being exported to the estuary during summer, decreasing the probability of DIN induced estuarine algal blooms (Anderson et al., 2008).

## 4. Conclusions

Our study provides valuable insights into the long-term effects of inorganic and organic pollution reduction and the tight coupling with the ecosystem functions of DIN retention and metabolism within large rivers. The shift from a heterotrophic-dominated to an autotrophic-dominated DIN retention regime and the associated changes in the seasonal patterns have implications for the carbon cycle and algal blooms in downstream ecosystems.

Our findings highlight the importance of considering different dimensions of integrative ecosystem functions (metabolism, DIN retention) when assessing long-term ecological changes in rivers, such as eutrophication. Dissolved oxygen





410 concentration time series alone are sufficient to support our findings of an autotrophic to heterotrophic regime shift, but estimates of GPP, ER, and DIN retention were required to support a quantitative assessment of the magnitude and consequences of this shift. The discovery of decoupled responses of ER and GPP to improvements in water quality offers new insights on the time scales of aquatic ecosystem responses to changing external forcing and informs realistic estimates for the efficiency of nutrient management and the achievement of environmental objectives.

### Competing interests

415 The contact author has declared that none of the authors has any competing interests.

### Acknowledgments

420 AW was funded by the Helmholtz-International Research School "Trajectories towards Water Security" (TRACER, grand no. HIRS-0017).

### Author contribution statement

Conceptualization:	all Authors
Methodology:	AW, JWJ
Data curation:	AW
425 Formal analyses and investigation:	AW, JWJ
Writing (original draft):	AW
Writing (review and editing):	AW, JWJ, DB
Supervision:	JWJ, DB

### 430 Data & Code availability

Q, DIN, temperature and DO time series can be downloaded from the FGG Elbe webportal [www.elbe-datenportal.de/FisFggElbe/](http://www.elbe-datenportal.de/FisFggElbe/).

Code is available from the author upon reasonable request.



## References

- 435 Aberle, J., Nikora, V., Henning, M., Ettmer, B., Hentschel, B., 2010. Statistical characterization of bed roughness due to bed forms: A field study in the Elbe River at Aken, Germany. *Water Resources Research* 46. <https://doi.org/10.1029/2008WR007406>
- Adams, M.S., Ballin, U., Gaumert, T., Hale, B.W., Kausch, H., Kruse, R., 2001a. Monitoring selected indicators of  
440 ecological change in the Elbe River since the fall of the Iron Curtain. *Conservation* 28, 333–344. <https://doi.org/10.1017/S0376892901000364>
- Arroita, M., Elozegi, A., Hall Jr., R.O., 2019. Twenty years of daily metabolism show riverine recovery following sewage abatement. *Limnology and Oceanography* 64, S77–S92. <https://doi.org/10.1002/lno.11053>
- 445 Ballard, T.C., Sinha, E., Michalak, A.M., 2019. Long-Term Changes in Precipitation and Temperature Have Already Impacted Nitrogen Loading. *Environmental Science & Technology* 53, 5080–5090. <https://doi.org/10.1021/acs.est.8b06898>
- Bauerkaemper, A., 2004. The Industrialization of Agriculture and its Consequences for the Natural Environment: An Inter-  
450 German Comparative Perspective. *Historical Social Research / Historische Sozialforschung* 29, 124–149.
- Bergbusch, N.T., Hayes, N.M., Simpson, G.L., Leavitt, P.R., 2021. Unexpected shift from phytoplankton to periphyton in eutrophic streams due to wastewater influx. *Limnology and Oceanography* 66, 2745–2761. <https://doi.org/10.1002/lno.11786>
- 455 Berggren, M., Lapierre, J.-F., del Giorgio, P.A., 2012. Magnitude and regulation of bacterioplankton respiratory quotient across freshwater environmental gradients. *ISME J* 6, 984–993. <https://doi.org/10.1038/ismej.2011.157>
- Bernhardt, E.S., Savoy, P., Vlah, M.J., Appling, A.P., Koenig, L.E., Hall, R.O., Arroita, M., Blaszczyk, J.R., Carter, A.M., Cohen, M., Harvey, J.W., Heffernan, J.B., Helton, A.M., Hosen, J.D., Kirk, L., McDowell, W.H., Stanley, E.H., Yackulic, C.B., Grimm, N.B., 2022. Light and flow regimes regulate the metabolism of rivers. *Proceedings of the National Academy of Sciences* 119, e2121976119. <https://doi.org/10.1073/pnas.2121976119>
- 460 Bertuzzo, E., Helton, A.M., Hall, R.O., Battin, T.J., 2017. Scaling of dissolved organic carbon removal in river networks. *Advances in Water Resources* 110, 136–146. <https://doi.org/10.1016/j.advwatres.2017.10.009>
- 465



- Bianchi, T.S., DiMarco, S.F., Cowan, J.H., Hetland, R.D., Chapman, P., Day, J.W., Allison, M.A., 2010. The science of hypoxia in the Northern Gulf of Mexico: A review. *Science of The Total Environment* 408, 1471–1484. <https://doi.org/10.1016/j.scitotenv.2009.11.047>
- 470 Booker, D.J., Dunbar, M.J., 2008. Predicting river width, depth and velocity at ungauged sites in England and Wales using multilevel models. *Hydrological Processes* 22, 4049–4057. <https://doi.org/10.1002/hyp.7007>
- Cavaliere, E., Baulch, H.M., 2019. Winter nitrification in ice-covered lakes. *PLOS ONE* 14, e0224864. <https://doi.org/10.1371/journal.pone.0224864>
- 475 Cejudo, E., Taylor, W., Schiff, S., 2020. Epilithic algae from an urban river preferentially use ammonium over nitrate. undefined.
- Chapra, S.C., Di Toro, D.M., 1991. Delta Method For Estimating Primary Production, Respiration, And Reaeration In  
480 Streams. *Journal of Environmental Engineering* 117, 640–655. [https://doi.org/10.1061/\(ASCE\)0733-9372\(1991\)117:5\(640\)](https://doi.org/10.1061/(ASCE)0733-9372(1991)117:5(640))
- Collos, Y., Harrison, P.J., 2014a. Acclimation and toxicity of high ammonium concentrations to unicellular algae. *Marine Pollution Bulletin* 80, 8–23. <https://doi.org/10.1016/j.marpolbul.2014.01.006>
- 485 del Giorgio, P.A., Cole, J.J., Cimleris, A., 1997. Respiration rates in bacteria exceed phytoplankton production in unproductive aquatic systems. *Nature* 385, 148–151. <https://doi.org/10.1038/385148a0>
- Deutsch, B., Voss, M., Fischer, H., 2009. Nitrogen transformation processes in the Elbe River: Distinguishing between assimilation and denitrification by means of stable isotope ratios in nitrate. *Aquatic Sciences* 71, 228–237.  
490 <https://doi.org/10.1007/s00027-009-9147-9>
- Diamond, J.S., Moatar, F., Cohen, M.J., Poirel, A., Martinet, C., Maire, A., Pinay, G., 2022a. Metabolic regime shifts and ecosystem state changes are decoupled in a large river. *Limnology & Oceanography* 67. <https://doi.org/10.1002/lno.11789>
- 495 Duffie, J.A., Beckman, W.A., 2013. *Solar Engineering of Thermal Processes*. John Wiley & Sons.
- Escoffier, N., Bensoussan, N., Vilmin, L., Flipo, N., Rocher, V., David, A., Métivier, F., Groleau, A., 2018. Estimating ecosystem metabolism from continuous multi-sensor measurements in the Seine River. *Environ Sci Pollut Res* 25, 23451–23467. <https://doi.org/10.1007/s11356-016-7096-0>



- 500 Filoso, S., Palmer, M.A., 2011. Assessing stream restoration effectiveness at reducing nitrogen export to downstream waters. *Ecological Applications* 21, 1989–2006. <https://doi.org/10.1890/10-0854.1>
- Gao, B., 1996. NDWI—A normalized difference water index for remote sensing of vegetation liquid water from space. *Remote Sensing of Environment* 58, 257–266. [https://doi.org/10.1016/S0034-4257\(96\)00067-3](https://doi.org/10.1016/S0034-4257(96)00067-3)
- 505 Godwin, C.M., Cotner, J.B., 2018. What intrinsic and extrinsic factors explain the stoichiometric diversity of aquatic heterotrophic bacteria? *ISME J* 12, 598–609. <https://doi.org/10.1038/ismej.2017.195>
- Guhr, H., Karrasch, B., Spott, D., 2000. Shifts in the Processes of Oxygen and Nutrient Balances in the River Elbe since the  
510 Transformation of the Economic Structure. *Acta Hydrochimica et Hydrobiologica* 28, 155–161. [https://doi.org/10.1002/1521-401x\(200003\)28:3<155::aid-aheh155>3.0.co;2-r](https://doi.org/10.1002/1521-401x(200003)28:3<155::aid-aheh155>3.0.co;2-r)
- Hall, R.Jr.O., Tank, J.L., 2003. Ecosystem metabolism controls nitrogen uptake in streams in Grand Teton National Park, Wyoming. *Limnology and Oceanography* 48, 1120–1128. <https://doi.org/10.4319/lo.2003.48.3.1120>
- 515 Hall, R.O., Tank, J.L., Baker, M.A., Rosi-Marshall, E.J., Hotchkiss, E.R., 2016. Metabolism, Gas Exchange, and Carbon Spiraling in Rivers. *Ecosystems* 19, 73–86. <https://doi.org/10.1007/s10021-015-9918-1>
- Hardenbicker, P., Rolinski, S., Weitere, M., Fischer, H., 2014. Contrasting long-term trends and shifts in phytoplankton  
520 dynamics in two large rivers. *International Review of Hydrobiology* 99, 287–299. <https://doi.org/10.1002/iroh.201301680>
- Heffernan, J.B., Cohen, M.J., 2010. Direct and indirect coupling of primary production and diel nitrate dynamics in a subtropical spring-fed river. *Limnology and Oceanography* 55, 677–688. <https://doi.org/10.4319/lo.2010.55.2.0677>
- 525 Hillebrand, G., Hardenbicker, P., Fischer, H., Otto, W., Vollmer, S., 2018. Dynamics of total suspended matter and phytoplankton loads in the river Elbe. *Journal of Soils and Sediments*. <https://doi.org/10.1007/s11368-018-1943-1>
- Hirsch, R.M., Moyer, D.L., Archfield, S.A., 2010. Weighted Regressions on Time, Discharge, and Season (WRTDS), with an Application to Chesapeake Bay River Inputs1. *JAWRA Journal of the American Water Resources Association* 46, 857–  
530 880. <https://doi.org/10.1111/j.1752-1688.2010.00482.x>
- IKSE, 2010. Abschlussbericht Aktionsprogramm Elbe 1996 – 2010.



535 IKSE, 2005. {Die Elbe und ihr Einzugsgebiet: Ein geographisch-hydrologischer und wasserwirtschaftlicher Überblick}.  
Internationale Kommission zum Schutz der Elbe (IKSE).

Jarvie, H.P., Macrae, M.L., Anderson, M., Celmer-Repin, D., Plach, J., King, S.M., 2022. River metabolic fingerprints and regimes reveal ecosystem responses to enhanced wastewater treatment. *Journal of Environmental Quality* 51, 811–825.  
<https://doi.org/10.1002/jeq2.20401>

540

Kamjunke, N., Beckers, L.-M., Herzsprung, P., von Tümpling, W., Lechtenfeld, O., Tittel, J., Risse-Buhl, U., Rode, M., Wachholz, A., Kallies, R., 2022. Lagrangian profiles of riverine autotrophy, organic matter transformation, and micropollutants at extreme drought. *Science of The Total Environment* 828, 154243.

545 Kamjunke, N., Rode, M., Baborowski, M., Kunz, J.V., Zehner, J., Borchardt, D., Weitere, M., 2021. High irradiation and low discharge promote the dominant role of phytoplankton in riverine nutrient dynamics. *Limnology and Oceanography* n/a.  
<https://doi.org/10.1002/lno.11778>

Kelly, M.C., Zeglin, L.H., Husic, A., Burgin, A.J., 2021. High Supply, High Demand: A Fertilizer Waste Release Impacts Nitrate Uptake and Metabolism in a Large River. *JGR Biogeosciences* 126. <https://doi.org/10.1029/2021JG006469>

Lehmann, A., Rode, M., 2001. Long-term behaviour and cross-correlation water quality analysis of the river Elbe, Germany. *Water Research* 35, 2153–2160. [https://doi.org/10.1016/S0043-1354\(00\)00488-7](https://doi.org/10.1016/S0043-1354(00)00488-7)

555 Lutz, S., Ebeling, P., Musolff, A., Nguyen, T., Sarrazin, F., Van Meter, K., Basu, N., Fleckenstein, J., Attinger, S., Kumar, R., 2022. Pulling the Rabbit out of the Hat: Unravelling Hidden Nitrogen Legacies in Catchment-Scale Water Quality Models. *Hydrological Processes* 36. <https://doi.org/10.1002/hyp.14682>

560 Markovic, D., Scharfenberger, U., Schmutz, S., Pletterbauer, F., Wolter, C., 2013. Variability and alterations of water temperatures across the Elbe and Danube River Basins. *Climatic Change* 119, 375–389. <https://doi.org/10.1007/s10584-013-0725-4>

Middelburg, J., Nieuwenhuize, J., 2000. Nitrogen uptake by heterotrophic bacteria and phytoplankton in the nitrate-rich Thames estuary. *Mar. Ecol. Prog. Ser.* 203, 13–21. <https://doi.org/10.3354/meps203013>

565



- Modi, P., Revel, M., Yamazaki, D., 2022. Multivariable Integrated Evaluation of Hydrodynamic Modeling: A Comparison of Performance Considering Different Baseline Topography Data. *Water Resources Research* 58. <https://doi.org/10.1029/2021WR031819>
- 570 Mundersbach, C., Bender, J., Netzel, F., 2016. An analysis of changes in flood quantiles at the gauge Neu Darchau (Elbe River) from 1875 to 2013. *Proc. IAHS* 373, 193–199. <https://doi.org/10.5194/piahs-373-193-2016>
- Netzband, A., Reincke, H., Bergemann, M., 2002. The river elbe. *Journal of Soils and Sediments* 2. <https://doi.org/10.1007/BF02988462>
- 575 Pathak, D., Hutchins, M., Brown, L.E., Loewenthal, M., Scarlett, P., Armstrong, L., Nicholls, D., Bowes, M., Edwards, F., Old, G., 2022. High-resolution water-quality and ecosystem-metabolism modeling in lowland rivers. *Limnology and Oceanography* 67, 1313–1327. <https://doi.org/10.1002/lno.12079>
- 580 Petersen, W., Callies, U., 2002. Assessment of Primary Production by Statistical Analysis of Water-quality Data. *Acta hydrochimica et hydrobiologica* 30, 34–40. [https://doi.org/10.1002/1521-401X\(200207\)30:1<34::AID-AHEH34>3.0.CO;2-M](https://doi.org/10.1002/1521-401X(200207)30:1<34::AID-AHEH34>3.0.CO;2-M)
- Powers, S.M., Baulch, H.M., Hampton, S.E., Labou, S.G., Lottig, N.R., Stanley, E.H., 2017. Nitrification contributes to winter oxygen depletion in seasonally frozen forested lakes. *Biogeochemistry* 136, 119–129. <https://doi.org/10.1007/s10533-017-0382-1>
- 585 Rasmussen, J.J., Baattrup-Pedersen, A., Riis, T., Friberg, N., 2011. Stream ecosystem properties and processes along a temperature gradient. *Aquat Ecol* 45, 231–242. <https://doi.org/10.1007/s10452-010-9349-1>
- 590 Rier, S.T., Stevenson, R.J., 2002. Effects of light, dissolved organic carbon, and inorganic nutrients [2pt] on the relationship between algae and heterotrophic bacteria in stream periphyton. *Hydrobiologia* 489, 179–184. <https://doi.org/10.1023/A:1023284821485>
- 595 Ritz, S., Dähnke, K., Fischer, H., 2017. Open-channel measurement of denitrification in a large lowland river. *Aquat Sci* 80, 11. <https://doi.org/10.1007/s00027-017-0560-1>
- Ritz, S., Fischer, H., 2019a. A Mass Balance of Nitrogen in a Large Lowland River (Elbe, Germany). *Water* 11, 2383. <https://doi.org/10.3390/w11112383>



600

Rode, M., Halbedel Née Angelstein, S., Anis, M.R., Borchardt, D., Weitere, M., 2016. Continuous In-Stream Assimilatory Nitrate Uptake from High-Frequency Sensor Measurements. *Environ Sci Technol* 50, 5685–5694. <https://doi.org/10.1021/acs.est.6b00943>

605

Salvatier, J., Wiecki, T.V., Fonnesbeck, C., 2016. Probabilistic programming in Python using PyMC3. *PeerJ Comput. Sci.* 2, e55. <https://doi.org/10.7717/peerj-cs.55>

610

Savoy, P., Appling, A.P., Heffernan, J.B., Stets, E.G., Read, J.S., Harvey, J.W., Bernhardt, E.S., 2019. Metabolic rhythms in flowing waters: An approach for classifying river productivity regimes. *Limnology and Oceanography* 64, 1835–1851. <https://doi.org/10.1002/lno.11154>

615

Scharfe, M., Callies, U., Blöcker, G., Petersen, W., Schroeder, F., 2009. A simple Lagrangian model to simulate temporal variability of algae in the Elbe River. *Ecological Modelling* 220, 2173–2186. <https://doi.org/10.1016/j.ecolmodel.2009.04.048>

620

Seitzinger, S.P., Styles, R.V., Boyer, E.W., Alexander, R.B., Billen, G., Howarth, R.W., Mayer, B., Breemen, N.V., 2002. Nitrogen retention in rivers: Model development and application to watersheds in the northeastern U.S.A., in: *Biogeochemistry*. Springer, pp. 199–237. <https://doi.org/10.1023/A:1015745629794>

625

Serra-Llobet, A., Jähnig, S.C., Geist, J., Kondolf, G.M., Damm, C., Scholz, M., Lund, J., Opperman, J.J., Yarnell, S.M., Pawley, A., Shader, E., Cain, J., Zingraff-Hamed, A., Grantham, T.E., Eisenstein, W., Schmitt, R., 2022. Restoring Rivers and Floodplains for Habitat and Flood Risk Reduction: Experiences in Multi-Benefit Floodplain Management From California and Germany. *Frontiers in Environmental Science* 9. <https://doi.org/10.3389/fenvs.2021.778568>

630

Sherman, E., Moore, J.K., Primeau, F., Tanouye, D., 2016. Temperature influence on phytoplankton community growth rates. *Global Biogeochemical Cycles* 30, 550–559. <https://doi.org/10.1002/2015GB005272>  
Snell, M.A., Barker, P.A., surridge, B.W.J., Benskin, C.H.M., Barber, N., Reaney, M., tych, W., Mindham, D., Large, A.R.G., Burke, S., Haygarth, M., 2019. Strong and recurring seasonality revealed within stream diatom assemblages. *Scientific Reports* 9. <https://doi.org/10.1038/s41598-018-37831-w>

630

Trentman, M.T., Tank, J.L., Davis, R.T., Hanrahan, B.R., Mahl, U.H., Roley, S.S., 2022. Watershed-scale Land Use Change Increases Ecosystem Metabolism in an Agricultural Stream. *Ecosystems* 25, 441–456. <https://doi.org/10.1007/s10021-021-00664-2>



- 635 Triska, F.J., Jackman, A.P., Duff, J.H., Avanzino, R.J., 1994. Ammonium sorption to channel and riparian sediments: A transient storage pool for dissolved inorganic nitrogen. *Biogeochemistry* 26, 67–83. <https://doi.org/10.1007/BF02182880>
- Tromboni, F., Hotchkiss, E.R., Schechner, A.E., Dodds, W.K., Poulson, S.R., Chandra, S., 2022. High rates of daytime river metabolism are an underestimated component of carbon cycling. *Commun Earth Environ* 3, 270.  
640 <https://doi.org/10.1038/s43247-022-00607-2>
- Vannote, R.L., Minshall, G.W., Cummins, K.W., Sedell, J.R., Cushing, C.E., 1980. The River Continuum Concept. *Can. J. Fish. Aquat. Sci.* 37, 130–137. <https://doi.org/10.1139/f80-017>
- 645 Virtanen, P., Gommers, R., Oliphant, T.E., Haberland, M., Reddy, T., Cournapeau, D., Burovski, E., Peterson, P., Weckesser, W., Bright, J., van der Walt, S.J., Brett, M., Wilson, J., Millman, K.J., Mayorov, N., Nelson, A.R.J., Jones, E., Kern, R., Larson, E., Carey, C.J., Polat, İ., Feng, Y., Moore, E.W., VanderPlas, J., Laxalde, D., Perktold, J., Cimrman, R., Henriksen, I., Quintero, E.A., Harris, C.R., Archibald, A.M., Ribeiro, A.H., Pedregosa, F., van Mulbregt, P., SciPy 1.0 Contributors, 2020. SciPy 1.0: Fundamental Algorithms for Scientific Computing in Python. *Nature Methods* 17, 261–272.  
650 <https://doi.org/10.1038/s41592-019-0686-2>
- Wachholz, A., Jawitz, J.W., Büttner, O., Jomaa, S., Merz, R., Yang, S., Borchardt, D., 2022. Drivers of multi-decadal nitrate regime shifts in a large European catchment. *Environ. Res. Lett.* 17, 064039. <https://doi.org/10.1088/1748-9326/ac6f6a>
- 655 Wang, J., Xia, X., Liu, S., Zhang, S., Zhang, L., Jiang, C., Zhang, Z., Xin, Y., Chen, X., Huang, J., Bao, J., McDowell, W.H., Michalski, G., Yang, Z., Xia, J., 2022. The Dominant Role of the Water Column in Nitrogen Removal and N<sub>2</sub>O Emissions in Large Rivers. *Geophysical Research Letters* 49. <https://doi.org/10.1029/2022GL098955>
- Wanninkhof, R., 1992. Relationship between wind speed and gas exchange over the ocean. *Journal of Geophysical Research: Oceans* 97, 7373–7382. <https://doi.org/10.1029/92JC00188>
- 660 Weiss, R.F., 1970. The solubility of nitrogen, oxygen and argon in water and seawater. *Deep Sea Research and Oceanographic Abstracts* 17, 721–735. [https://doi.org/10.1016/0011-7471\(70\)90037-9](https://doi.org/10.1016/0011-7471(70)90037-9)
- 665 Zhang, X., Yang, X., Hensley, R., Lorke, A., Rode, M., 2023. Disentangling In-Stream Nitrate Uptake Pathways Based on Two-Station High-Frequency Monitoring in High-Order Streams. *Water Resources Research* 59, e2022WR032329. <https://doi.org/10.1029/2022WR032329>